

## Quantum Zeno Effects from Measurement Controlled Qubit-Bath Interactions

P. M. Harrington,<sup>1</sup> J. T. Monroe,<sup>1</sup> and K. W. Murch<sup>1,2,\*</sup>

<sup>1</sup>*Department of Physics, Washington University, Saint Louis, Missouri 63130, USA*

<sup>2</sup>*Institute for Materials Science and Engineering, Saint Louis, Missouri 63130, USA*

(Received 24 March 2017; published 14 June 2017)

The Zeno and anti-Zeno effects are features of measurement-driven quantum evolution where frequent measurement inhibits or accelerates the decay of a quantum state. Either type of evolution can emerge depending on the system-environment interaction and measurement method. In this experiment, we use a superconducting qubit to map out both types of Zeno effect in the presence of structured noise baths and variable measurement rates. We observe both the suppression and acceleration of qubit decay as repeated measurements are used to modulate the qubit spectrum causing the qubit to sample different portions of the bath. We compare the Zeno effects arising from dispersive energy measurements and purely dephasing “quasimeasurements,” showing energy measurements are not necessary to accelerate or suppress the decay process.

DOI: 10.1103/PhysRevLett.118.240401

A projective measurement should reset the clock of a decay process, reinitializing the system to its excited state and therefore inhibiting decay in a variety of situations ranging from nuclear physics [1] to optical lattices [2]. The suppression of a decay process—and more broadly quantum evolution—by frequent measurement is referred to as the “Zeno effect” [3]. The fact that the Zeno effect in decay processes is almost universally negligible is evident by considering Fermi’s golden rule for determining a decay rate: the decay rate depends on the density of states only at the transition frequency and repeated measurement effectively samples a larger range of frequencies in the calculation. If the bath is white on the probed band, then the decay rate is unchanged. Therefore, the Zeno effect will only occur under the special circumstance where the noise spectral density varies quickly over the probed band. Moreover, the opposite “anti-Zeno effect,” where frequent measurements accelerate decay, is predicted to be a more ubiquitous phenomenon [4–6]. Here we perform a detailed study of both Zeno effects using a superconducting qubit as an emitter coupled to a transmission line with a tunable structured bath. Frequent measurements alter the qubit-bath interaction leading to both accelerated and suppressed decay. Our study expands on the role of measurement in the Zeno effects and highlights new ways to control quantum evolution with tunable bath interactions [7].

The original development of the Zeno effect predicted the inhibition of particle decay and nonexponential dynamics due to time-evolution interruption from frequent observations [3]. The general case for any quantum system under continuous measurement, dubbed the “watchdog-effect” [8], was explained in terms of cancellation of wave function coherence caused from measurement induced perturbations, thus slowing evolution from an initial state [9]. The first experimental measurements of the Zeno effect, conducted

with trapped ions [10], incited much discourse on the nature of measurement, the essential features of the Zeno effect, and how the effect compares to simple perturbation dynamics due to external coupling [11,12]. In recent years, the effect has been generalized as any disruption of the unitary evolution due to projectionlike interactions with an external system [13], and it has also been suggested that Zeno-like dynamics can arise from unitary (nonprojective) dynamics alone [14–16]. The anti-Zeno effect occurs when frequent measurements accelerate a decay process and was first observed (along with the Zeno effect) in a tunneling experiment with a cold atomic gas [17].

In contrast to previous work [2,10,17], our experiment focuses on a single-quantum system, where ensemble averaging occurs only after data collection [18]. While Zeno effects, and more broadly Zeno dynamics, have been studied with superconducting qubits [19–21], the anti-Zeno effect has not yet been studied at the level of a single-quantum system. In our experiment, we demonstrate how both types of Zeno effect arise from frequent projective energy measurements on a superconducting qubit. Furthermore, to examine the role of information for Zeno decay dynamics, we introduce a dephasing-only “measurement” method which does not cause measurement backaction in the energy basis.

Our system consists of a transmon circuit that is dispersively coupled to a three-dimensional waveguide cavity of frequency  $\omega_c/2\pi = 6.895$  GHz [Fig. 1(a)] [22,23]. The two lowest energy eigenstates  $\{|g\rangle, |e\rangle\}$  define a qubit with a transition frequency of  $\omega_{ge}/2\pi = 5.103$  GHz. The interaction Hamiltonian,  $H_{\text{int}}/\hbar = -\chi a^\dagger a \sigma_z$ , results in a qubit-state-dependent frequency shift of the cavity [Fig. 1(b)] [24]. Here,  $a^\dagger$  ( $a$ ) is the creation (annihilation) operator for the cavity resonance,  $\sigma_z$  is the Pauli spin operator which has the qubit energy states as an eigenbasis, and  $\chi/2\pi = -1.38$  MHz is the dispersive coupling rate. A probe that

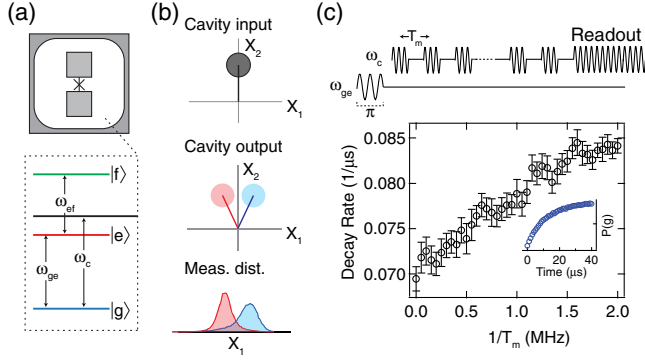


FIG. 1. Experimental setup. (a) The system consists of a transmon circuit dispersively coupled to a waveguide cavity, where the  $|g\rangle$  and  $|e\rangle$  states define the qubit and  $|f\rangle$  is an auxiliary state. (b) The qubit-cavity interaction results in a state-dependent phase shift on a probe near the cavity frequency,  $\omega_c$ , allowing the single-shot measurement of the qubit state. (c) A standard inversion recovery ( $T_1$ ) measurement (inset) is used to characterize the effect of repeated projective measurements. A slight increase in the decay rate as the intermeasurement time interval  $T_m$  is decreased is expected from the non-QND character of the measurement.

populates the cavity with an average intracavity photon number  $\bar{n}$  results in dispersive measurement of the qubit energy state characterized by a time scale  $\tau = \kappa / (16\bar{n}\eta\chi^2)$ , where  $\kappa/2\pi = 6.81$  MHz is the cavity linewidth and  $\eta = 0.014$  is the measurement quantum efficiency [25–27].

Since the measurement operator  $\sigma_z$  commutes with the Hamiltonian, this measurement is considered quantum nondemolition (QND). However, counter-rotating terms and noise mixing break the QND character of this measurement [28,29]. To analyze repeated measurements, we perform qubit lifetime measurements while applying 100 ns long probe pulses that occupy the cavity with  $\bar{n} = 9$  intracavity photons. If the probe photons were detected with unity quantum efficiency, then this measurement would distinguish between the energy eigenstates of the circuit with nearly unit fidelity. As such, we consider these measurements to be complete projective measurements, even though the paltry quantum efficiency of the setup inhibits our ability to record these measurements with exceedingly high fidelity. As shown in Fig. 1(c), the observed  $T_1$  of the qubit in the presence of these measurements does decrease, though we emphasize that this alteration of the decay rate is not a Zeno effect as it can easily be explained by considering the non-QND character of the measurement [28,29].

To study Zeno effects in this system, we introduce a structured thermal bath that alters the decay rate of the transmon circuit. We synthesize a bath of a Lorentzian amplitude spectrum from a white-noise source filtered by a low-pass LC filter resulting in a power spectrum with a 3-dB-width of 1 MHz. This low-frequency noise is up-converted to near the qubit transition,  $\omega_{ge}$ , via

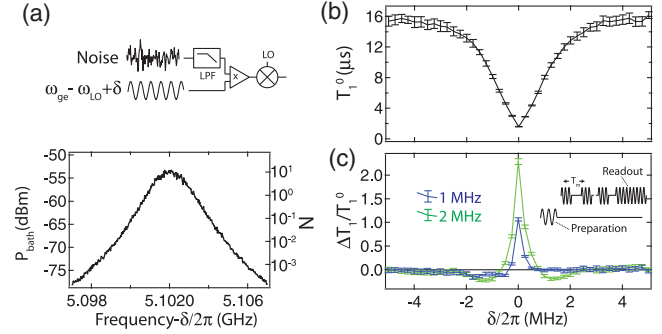


FIG. 2. Synthesized noise bath and Zeno effects. (a) A structured thermal noise bath is created from a filtered white-noise source mixed up to the qubit transition frequency. The bath is characterized by a Lorentzian squared power spectrum (shown here at the input plane of the dilution refrigerator), with a center frequency that is tunable from the low-frequency modulation  $\omega_{ge} - \omega_{LO} + \delta$ . (b) Inversion recovery measurements in the presence of the noise bath show how the thermal photons decrease the effective decay time when the bath is centered near the qubit transition. (c) The fractional change in the qubit  $T_1$  decay time,  $\Delta T_1 = (T_1 - T_1^0)/T_1^0$ , versus qubit-bath detuning, where  $T_1^0$  is the  $T_1$  time in the absence of additional measurement, as shown in (b). Repeated projective measurements, applied at a rate  $1/T_m = 2$  MHz (green) and  $1/T_m = 1$  MHz (blue), alter the coupling of the qubit to the bath. This either enhances (anti-Zeno effect, below the horizontal line) or suppresses (Zeno effect, above the horizontal line) the decay relative to the case without measurements.

single-sideband modulation [Fig. 2(a)]. This thermal photon bath induces stimulated emission and absorption of the qubit, modifying the decay rate. The strength of the bath coupling to the qubit transition is characterized by  $N$ , the average number of thermal photons. When the bath contains  $N$  thermal photons, the radiative decay time decreases as

$$T_1 = T_{1,\text{spont}} / (2N + 1) \quad (1)$$

where  $T_{1,\text{spont}} = 20 \mu\text{s}$  is the radiative decay time from spontaneous emission and  $N$  is the number of thermal photons coupling to the qubit transition [30,31].

To examine the effect of the synthesized noise bath on the qubit transition decay rate, we perform inversion recovery measurements for different detunings  $\delta$  between the bath center and the qubit transition. Figure 2(b) shows that reducing the detuning of the center frequency of the bath relative to the qubit transition decreases the  $T_1$  coherence time according to the bath’s power spectral density. We note that instead of injecting thermal photons into our system, the electromagnetic spectral density could be colored by the use of a “Purcell filter”—a shunting narrow-band notch filter that suppresses the vacuum fluctuations [32].

We now focus on how repeated measurements alter the coupling of the qubit to a structured thermal environment,

thereby reducing or enhancing decay. We can treat this with a simple theoretical model where the decay rate of the qubit is determined by the coupling of environmental modes to the qubit transition frequency. The decay rate is calculated by the overlap integral,

$$1/T_1 = 2\pi \int_{-\infty}^{+\infty} d\omega F(\omega, T_m) G(\omega) \quad (2)$$

where  $F(\omega, T_m)$  is the qubit transition spectral profile during measurement at a rate  $1/T_m$  and  $G(\omega)$  is the environment density of states [33]. In general, the qubit spectral profile is broadened upon measurement which results in a different weighted average over the environmental modes. Consequently, when  $G(\omega)$  varies in frequency, the qubit decay rate can increase or decrease due to measurement induced broadening of  $F(\omega, T_m)$ . Figure 2(c) displays the fractional change  $\Delta T_1 = (T_1 - T_1^0)/T_1^0$  of the qubit  $T_1$  times versus the bath detuning frequency for different measurement rates. Here  $T_1^0$  specifies the decay time for a specific bath detuning in the absence of additional measurement. We note that the effect of an increased measurement rate is twofold: the non-QND character of higher measurement rates results in shorter  $T_1$  times (as shown in Fig. 1), and the repeated measurements alter the coupling of the qubit to the synthesized noise bath. To isolate this second effect, we scale the measured  $T_1$  values to correct for the non-QND contribution to the measured decay rate, as described in the Supplemental Material [34]. Since the presence of photons in the cavity causes an ac Stark shift on the qubit transition, we have also shifted the bath detuning values slightly to make a ratiometric comparison to the no measurement case.

As illustrated by this comparison [Fig. 2(c)], the repeated measurements result in regions where the measured  $T_1$  time is decreased (anti-Zeno effect, below the horizontal line) and increased [Zeno effect, above the horizontal line in Fig. 2(c)] compared to the no measurement case.

Zeno effects occur because measurement backaction perturbs the system, thereby altering its coupling to the bath. The backaction of dispersive  $\sigma_z$  measurements can be understood by considering the interaction Hamiltonian,  $H_{\text{int}}/\hbar = -\chi a^\dagger a \sigma_z$ . On one hand, this interaction describes an ac Stark shift of the qubit transition frequency by intracavity photons. Fluctuations of the intracavity photon number lead to fluctuations of the qubit frequency and thus dephasing. On the other hand, the cavity probe accumulates information about the qubit state in the energy eigenbasis, inducing “spooky” backaction associated with wave function collapse [35]. During continuous measurement, both the mechanism of photon number fluctuations and the acquired qubit state information perturb the qubit [25,26,36], leading to dephasing [37,38]. The presence of these two types of backaction (pure dephasing versus eigenstate information) draws into question the role of

information. Is projection onto an eigenstate an essential component of the Zeno effects? Indeed, a recent proposal [33] has introduced the concept of a “quasimeasurement”—an interaction with the environment that does not necessarily accumulate information about the state—to clarify the role of wave function collapse in the Zeno effects.

Accordingly, we implement an alternative measurement scheme which only dephases rather than accumulates information about the qubit state. In the proposal [33], a drive excites the qubit to an auxiliary state which rapidly decays through spontaneous emission [Fig. 3(a)]. This sequence implements a quasimeasurement: if the qubit is in the  $|e\rangle$  state the system will emit a photon, making a projective measurement in the energy basis. Here, we extend this proposal to perform a dephasing-only “measurement,” where no information about the energy state is acquired. To do this, we apply a rotation  $R_{\theta_1}^\pi$  on the  $\omega_{ef}$  transition to excite the circuit from  $|e\rangle$  to  $|f\rangle$  and then apply a second rotation  $R_{\theta_2}^\pi$  to return the circuit to the  $|e\rangle$  state. These two rotations result in an accumulated Berry phase [39–42] on the state  $|e\rangle$ . To characterize this Berry phase, we perform a Ramsey measurement as shown in Fig. 3(b). The Ramsey measurements show that the rotations imprint a specific phase evolution on the qubit state related to the phase difference of the two rotations. By randomizing the Berry phase, this interaction completely dephases the qubit state. Furthermore, because the rotations are conducted with a classical drive, no information of the qubit’s energy state is acquired in the interaction. These “dephasing measurements” are similar to the dispersive

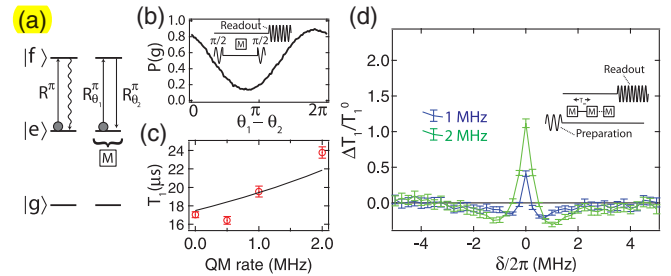


FIG. 3. **Dephasing measurements.** (a) The proposed quasimeasurement from [33] involves excitation to an auxiliary state and spontaneous decay. An alternative, dephasing, measurement uses a second  $\pi$  rotation to return the system to the  $|e\rangle$  state. (b) A Ramsey measurement on the qubit state to characterize the effect of the dephasing measurement. The phase difference of the two rotations in the dephasing measurement imprints a Berry phase on the state  $|e\rangle$ . Thus by randomizing the Berry phase, the interaction dephases the qubit. (c) Measured  $T_1$  times for different measurement rates in the absence of the synthesized noise bath. The black line indicates the expected systematic shift in the measured  $T_1$  time due to the time the circuit spends outside of the qubit manifold [34]. (d) Fractional change in the qubit  $T_1$  decay times in the presence of the synthesized noise bath for different qubit-bath detunings and different measurement rates.

energy measurements, where entanglement between the qubit and environment, and subsequent measurement of the environment, produces a random (owing to the quantum fluctuations of environment) perturbation on the qubit. For dephasing measurements, however, the perturbation is imprinted on the qubit by the relative phase of the rotations. The quasimeasurements do not acquire information of energy state populations but instead only dephase the state in the energy eigenbasis.

In the experiment, the dephasing measurements are implemented with two Gaussian pulses ( $\sigma = 10$  ns) on the  $\omega_{ef}$  transition separated by 67 ns. The relative phase between the two pulses is chosen from a pseudorandom number generator. Because each dephasing measurement takes the circuit out of the qubit state manifold, repeated measurements change the effective decay time as shown in Fig. 3(c), where the solid line indicates the expected dependence on the measured  $T_1$  based on the dephasing measurement rate [34].

We now return to our investigation of the Zeno effects. In Fig. 3(d), we display the fractional change in  $T_1$  versus bath detuning, repeating the same experimental sequence as in Fig. 2(c), but we have replaced the dispersive  $\sigma_z$  measurements with dephasing quasimeasurements. Here we have our central result: the quasimeasurement scheme exhibits the same decay time pattern as dispersive energy measurements when the bath spectrum is located at specific detunings from the qubit transition. For increasing measurement rates, we find suppressed decay (Zeno effect, above the horizontal line) when the bath spectrum is near the qubit transition and enhanced decay (anti-Zeno effect, below the horizontal line) when the bath is further detuned. At higher quasimeasurement rates the Zeno effects become more drastic. Our data show that dephasing measurements induce Zeno effects in a comparable way to projective  $\sigma_z$  measurements.

To probe how the repeated measurements alter the qubit-bath coupling we perform continuous wave spectroscopy of the qubit transition. Accordingly, a weak probe is applied at a variable frequency for a duration of  $80 \mu\text{s}$  before a projective measurement determines the excited state population. Figure 4 shows the final excited state population as a function of probe frequency for different measurement rates. By increasing measurement rates, we broaden and modulate the qubit transition. Dispersive measurements also result in a slight ac Stark shift of the transition to lower frequencies. The spectroscopy clearly shows how both dispersive and dephasing measurements perturb the qubit transition similarly, such that Zeno effects can arise depending on the spectral properties of the electromagnetic environment.

The Zeno and anti-Zeno effects occur from an emitter decoupling from or coupling to its environment. When random measurement perturbations broaden the emitter's resonance profile, the emitter samples more or less of the

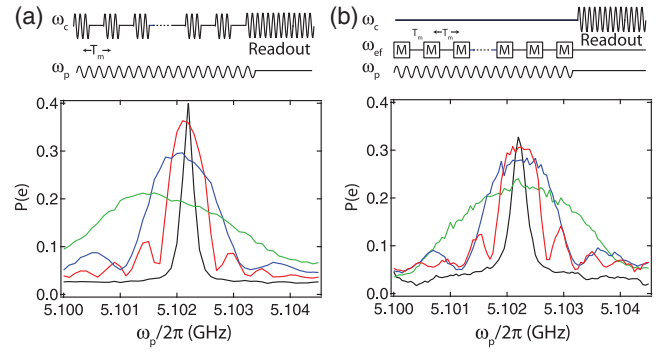


FIG. 4. Spectroscopy. A continuous weak probe at frequency  $\omega_p$  is applied for a duration of  $80 \mu\text{s}$  followed by a projective measurement. The power-broadened qubit transition frequency is revealed as an increase in the final excited state population (black traces). To probe the effects of dispersive (a) and quasimeasurements (b), we apply these measurements at different rates: 0.5, 1, and 2 MHz (red, blue, and green, respectively).

bath depending on the spectral density of states. Counter to the original conception of Zeno effects, the measurements that induce broadening of the emitter's transition do not need to acquire information about the system energy state, but should simply dephase the quantum state.

This experiment demonstrates tools for quantum state engineering through the interplay of radiative decay (dissipative bath interactions), dispersive interactions (projective  $\sigma_z$  measurement), and perturbation by a classical drive (dephasing from quasimeasurement). These methods can be extended to higher dimensional quantum systems to create Zeno dynamics [21,43–49], where measurement restricts state evolution to certain subspaces.

We thank D. Tan for sample fabrication, as well as M. Naghiloo, S. Hacoheh-Gourgy, and P. Kwiat for discussions. We acknowledge primary research support from NSF Grant No. PHY-1607156 and ONR Grant No. 12114811. This research used facilities at the Institute of Materials Science and Engineering at Washington University. K. W. M. acknowledges support from the Sloan Foundation.

\*Corresponding author.

murch@physics.wustl.edu

- [1] A. M. Lane, *Phys. Lett. A* **99**, 359 (1983).
- [2] Y. S. Patil, S. Chakram, and M. Vengalattore, *Phys. Rev. Lett.* **115**, 140402 (2015).
- [3] B. Misra and E. C. G. Sudarshan, *J. Math. Phys. (N.Y.)* **18**, 756 (1977).
- [4] B. Kaulakys and V. Gontis, *Phys. Rev. A* **56**, 1131 (1997).
- [5] A. G. Kofman and G. Kurizki, *Nature (London)* **405**, 546 (2000).
- [6] P. Facchi, H. Nakazato, and S. Pascazio, *Phys. Rev. Lett.* **86**, 2699 (2001).
- [7] J. F. Poyatos, J. I. Cirac, and P. Zoller, *Phys. Rev. Lett.* **77**, 4728 (1996).

- [8] K. Kraus, *Found. Phys.* **11**, 547 (1981).
- [9] A. Peres, *Am. J. Phys.* **48**, 931 (1980).
- [10] W.M. Itano, D.J. Heinzen, J.J. Bollinger, and D.J. Wineland, *Phys. Rev. A* **41**, 2295 (1990).
- [11] L. E. Ballentine, *Phys. Rev. A* **43**, 5165 (1991).
- [12] W.M. Itano, D.J. Heinzen, J.J. Bollinger, and D.J. Wineland, *Phys. Rev. A* **43**, 5168 (1991).
- [13] W. M. Itano, [arXiv:quant-ph/0612187](https://arxiv.org/abs/quant-ph/0612187).
- [14] S. Pascazio and M. Namiki, *Phys. Rev. A* **50**, 4582 (1994).
- [15] L. Viola and S. Lloyd, *Phys. Rev. A* **58**, 2733 (1998).
- [16] T. Nakanishi, K. Yamane, and M. Kitano, *Phys. Rev. A* **65**, 013404 (2001).
- [17] M. C. Fischer, B. Gutiérrez-Medina, and M. G. Raizen, *Phys. Rev. Lett.* **87**, 040402 (2001).
- [18] P. E. Toschek, *Europhys. Lett.* **102**, 20005 (2013).
- [19] K. Kakuyanagi, T. Baba, Y. Matsuzaki, H. Nakano, S. Saito, and K. Semba, *New J. Phys.* **17**, 063035 (2015).
- [20] D. H. Slichter, C. Müller, R. Vijay, S. J. Weber, A. Blais, and I. Siddiqi, *New J. Phys.* **18**, 053031 (2016).
- [21] L. Bretheau, P. Campagne-Ibarcq, E. Flurin, F. Mallet, and B. Huard, *Science* **348**, 776 (2015).
- [22] J. Koch, T. M. Yu, J. Gambetta, A. A. Houck, D. I. Schuster, J. Majer, A. Blais, M. H. Devoret, S. M. Girvin, and R. J. Schoelkopf, *Phys. Rev. A* **76**, 042319 (2007).
- [23] H. Paik, D. I. Schuster, L. S. Bishop, G. Kirchmair, G. Catelani *et al.*, *Phys. Rev. Lett.* **107**, 240501 (2011).
- [24] A. Wallraff, D. I. Schuster, A. Blais, L. Frunzio, M. H. Majer, S. M. Girvin, and R. J. Schoelkopf, *Phys. Rev. Lett.* **95**, 060501 (2005).
- [25] K. W. Murch, S. J. Weber, C. Macklin, and I. Siddiqi, *Nature (London)* **502**, 211 (2013).
- [26] M. Hatridge, S. Shankar, M. Mirrahimi, F. Schackert, K. Geerlings, T. Brecht, K. M. Sliwa, B. Abdo, L. Frunzio, S. M. Girvin *et al.*, *Science* **339**, 178 (2013).
- [27] S. J. Weber, A. Chantasri, J. Dressel, A. N. Jordan, K. W. Murch, and I. Siddiqi, *Nature (London)* **511**, 570 (2014).
- [28] D. H. Slichter, R. Vijay, S. J. Weber, S. Boutin, M. Boissonneault, J. M. Gambetta, A. Blais, and I. Siddiqi, *Phys. Rev. Lett.* **109**, 153601 (2012).
- [29] D. Sank, Z. Chen, M. Khezri, J. Kelly, R. Barends *et al.*, *Phys. Rev. Lett.* **117**, 190503 (2016).
- [30] C. W. Gardiner, *Phys. Rev. Lett.* **56**, 1917 (1986).
- [31] K. W. Murch, S. J. Weber, K. M. Beck, E. Ginossar, and I. Siddiqi, *Nature (London)* **499**, 62 (2013).
- [32] M. D. Reed, B. R. Johnson, A. A. Houck, L. DiCarlo, J. M. Chow, D. I. Schuster, L. Frunzio, and R. J. Schoelkopf, *Appl. Phys. Lett.* **96**, 203110 (2010).
- [33] Q. Ai, D. Xu, S. Yi, A. G. Kofman, C. P. Sun, and F. Nori, *Sci. Rep.* **3**, 1752 (2013).
- [34] See Supplemental Material at <http://link.aps.org/supplemental/10.1103/PhysRevLett.118.240401> for further details.
- [35] A. N. Korotkov, [arXiv:1111.4016](https://arxiv.org/abs/1111.4016).
- [36] G. de Lange, D. Ristè, M. J. Tiggelman, C. Eichler, L. Tornberg, G. Johansson, A. Wallraff, R. N. Schouten, and L. DiCarlo, *Phys. Rev. Lett.* **112**, 080501 (2014).
- [37] D. I. Schuster, A. Wallraff, A. Blais, L. Frunzio, R.-S. Huang, J. Majer, S. M. Girvin, and R. J. Schoelkopf, *Phys. Rev. Lett.* **94**, 123602 (2005).
- [38] M. Boissonneault, J. M. Gambetta, and A. Blais, *Phys. Rev. A* **79**, 013819 (2009).
- [39] M. V. Berry, *Proc. R. Soc. A* **392**, 45 (1984).
- [40] P. J. Leek, J. M. Fink, A. Blais, R. Bianchetti, M. Göppel *et al.*, *Science* **318**, 1889 (2007).
- [41] A. A. Abdumalikov Jr, J. M. Fink, K. Juliusson, M. Pechal, S. Berger, A. Wallraff, and S. Filipp, *Nature (London)* **496**, 482 (2013).
- [42] C. G. Yale, F. J. Heremans, B. B. Zhou, A. Auer, G. Burkard, and D. D. Awschalom, *Nat. Photonics* **10**, 184 (2016).
- [43] P. Facchi and S. Pascazio, *Phys. Rev. Lett.* **89**, 080401 (2002).
- [44] J. M. Raimond, C. Sayrin, S. Gleyzes, I. Dotsenko, M. Brune, S. Haroche, P. Facchi, and S. Pascazio, *Phys. Rev. Lett.* **105**, 213601 (2010).
- [45] J. M. Raimond, P. Facchi, B. Peaudecerf, S. Pascazio, C. Sayrin, S. Haroche, P. Facchi, and S. Pascazio, *Phys. Rev. A* **86**, 032120 (2012).
- [46] F. Schäfer, I. Herrera, S. Cherukattil, C. Lovecchio, F. S. Cataliotti, F. Caruso, and A. Smerzi, *Nat. Commun.* **5**, 3194 (2014).
- [47] A. Signoles, A. Facon, D. Grosso, I. Dotsenko, S. Haroche, J.-M. Raimond, M. Brune, and S. Gleyzes, *Nat. Phys.* **10**, 715 (2014).
- [48] G. Barontini, L. Hohmann, F. Haas, J. Estève, and J. Reichel, *Science* **349**, 1317 (2015).
- [49] Y. Lin, J. P. Gaebler, F. Reiter, T. R. Tan, R. Bowler, Y. Wan, A. Keith, E. Knill, S. Glancy, K. Coakley *et al.*, *Phys. Rev. Lett.* **117**, 140502 (2016).